Nuclear IGF-1R interacts with regulatory regions of chromatin, promoting RNA polymerase II recruitment and gene expression associated with advanced tumor stage.

Tamara Aleksic, Nicki Gray, Xiaoning Wu, Guillaume Rieunier, Eliot Osher, Jack Mills, Clare Verrill, Richard J. Bryant, Cheng Han, Kathryn Hutchinson, Adam G. Lambert, Rajeev Kumar, Freddie C. Hamdy, Ulrike Weyer-Czernilofsky, Michael P. Sanderson, Thomas Bogenrieder, Stephen Taylor, Valentine M. Macaulay.

This file contains Supplementary methods, Tables S1-S4 and Figures S1-S6.

See also Supplementary Table S5.xlsx.

Supplementary Methods

IGF-1R and JUN Immunohistochemistry (IHC)

Freshly cut 4 µm sections of FFPE diagnostic prostate cancer biopsies underwent IHC as described (1, 2). In brief, following antigen retrieval in 50 mM Tris, 2 mM EDTA pH 9.0 (2 min at 125°C, 10 min at 85°C), slides were incubated overnight at 4°C with rabbit monoclonal IGF-1Rβ antibody (Cell Signaling, 9750) or JUN antibody ab32137 (Abcam), and bound antibody was detected used the Rabbit HRP-Polymer Detection kit (Menarini diagnostics, MP-531-M3R100). Membrane, cytoplasmic and nuclear IGF-1R were scored blinded by specialist Uro-Pathologist CV for intensity (0, nil; 1, weak; 2, moderate; 3, heavy) and percentage (0%, nil; 1: 1-10%; 2: 11-50%; 3: 51-80%; 4: 81-100%) of tumor stained, generating immunoreactive scores (range 0-12) for membrane, cytoplasmic and nuclear IGF-1R. JUN IHC was performed on adjacent sections using the same method using antibody ab32137 (Abcam), and scored for total JUN signal using the same intensity/percentage scale.

ChIP and ChIP-seq

Serum-starved subconfluent DU145 and SK-N-MC cultures were treated with 50nM Long R3-IGF-1 (Sigma) for 30 min. Cells were fixed in 1% formaldehyde for 10 min at room temperature and the reaction quenched with 125 mM glycine. After washing with cold PBS, cells were scraped in PBS with protease inhibitor cocktail (Roche) and Phosphatase inhibitor Cocktails 2 and 3 (Sigma-Aldrich). Cell pellets containing ~50 x 10^6 cells per condition were snap-frozen, stored at -20°C and subjected to ChIP using the ChIP Assay Kit (17-295, Millipore) according to the manufacturer's instructions. Briefly, cell pellets were lysed in SDS lysis buffer (ChIP assay kit, Millipore, 17-295) with fresh protease inhibitors for 30 min on ice, and sonicated in a Bioruptor sonicator (Diagenode) to fragment genomic DNA. Then 1% of total DNA was saved to use as input DNA for normalisation in subsequent qPCR. The remaining lysates were pre-cleared by addition of 80 µl salmon sperm DNA/Protein A agarose slurry for 1h, followed by immunoprecipitation using 5-10 µg antibodies against IGF-1R (Cell Signaling, 3027), H3K4me1 (Abcam, ab8895), H3K4me3 (Abcam, ab8580), RNAPol2 (Abcam, ab5095), or IgG (Santa Cruz) as negative control. After overnight incubation at +4°C, antibody-bound protein-DNA complexes were collected with Protein A agarose beads and washed using low salt, high salt, LiCl and TE wash buffers from the ChIP assay kit (Millipore) according to the manufacturer's protocol. Precipitated chromatin was eluted from the beads by shaking in fresh elution buffer (1% SDS, 0.1M NaHCO3) for 15 min at room temperature, and de-cross-linked at 65°C overnight in the presence of 0.2M NaCl. Chromatin was treated with proteinase K (1h at 45°C), DNAs were phenol-chloroform extracted, ethanol precipitated overnight at -20°C and resuspended in nuclease-free water.

ChIP-seq was performed on duplicate independent IGF-1R and control (IgG) ChIPs, and individual samples of RNAPol2 and H3K4me1/3 ChIPs. DNAs were end-repaired, A-tailed and adapter-ligated before amplification and size selection. The prepared libraries underwent paired end sequencing on a HiSeq flow cell (Illumina) at Wellcome Trust Centre for Human Genetics, Oxford UK. Mapping of ChIP-Seq reads was done with Bowtie2 (3) aligned to the human reference genome (hg19) from UCSC. The aligned reads were analysed with MACS2 for peak calling (4), using the IgG DNA as background in each comparison. These softwares reported peaks with assigned FDR values and p-values that identify DNA regions with statistically significant binding enrichment. ChIP fragment depth (per bp per peak) was produced using Homer (http://homer.salk.edu/homer/ngs/quantification.html). TRANSFAC

(http://www.gene-regulation.com/pub/databases.html) was used to search IGF-1R-bound promoter sequences for motifs that represent binding sites of established transcription factors.

Validation of ChIP-seq identified peaks was performed on triplicate independent samples of DU145 cells using the ChIP protocol and antibodies as above, and qPCR as described below. These methods were also used to test for IGF-1R recruitment to promoters in fresh frozen prostate cancer tissue samples. Frozen tissues were minced on ice in ice-cold PBS, fixed in 1% Formaldehyde in PBS at room temperature for 20 min and quenched with 125 mM Glycine. Tissues were then homogenized in 500 µl SDS lysis buffer with protease inhibitors as above, using ceramic beads in a TissueLyser (Qiagen). Tissue homogenates were incubated on ice for 30 min, centrifuged (14,000g, 5 min, 4°C) and supernatants were snap-frozen and stored at -20°C. Lysates were thawed on ice, sonicated (Bioruptor sonicator) and analyzed by ChIP-qPCR as above.

JUN promoter reporter

We extracted genomic DNA from DU145 cells using the DNeasy kit (Qiagen) according to the manufacturers protocol. The proximal *JUN* promoter was amplified using Phusion polymerase (Promega) with primers JUN-F and JUN-R (Supplementary Table S1) by PCR (30 cycles, annealing temperature 69°C, extension time 1 min). The 1.4 kb PCR product and pNLCol2 reporter (Promega) were digested with XhoI and HindIII-HF (New England Biolabs), digested products were heat-treated (80°C, 20 min) and pNLCol2 vector treated with thermosensitive alkaline phosphatase (1 hr, 37°C). Gel-purified plasmid backbone was ligated with the *JUN* promoter fragment and positive colonies were identified by colony PCR using primers pNL-F and pNL-R (30 cycles, annealing temperature 68°C, extension time 1 min). The correct sequence of the cloned insert was confirmed by DNA sequencing (Source Bioscience).

DU145 cells were transfected with pNLCol2 JUN or pNLCol2 empty vector (EV) using Lipofectamine 3000 (Invitrogen) and 48 hr later selected with 500 µg/mL hygromycin, determined to be optimal following a DU145 hygromycin (0-1000 µg/mL) kill curve. Stable pNLCol2 JUN clones were screened for the presence of the ~1.4 kb *JUN* promoter by PCR using primers pNL-F and pNL-R as above, and by testing for luciferase activity in excess of that detected in EV transfectants, in luciferase assays using ONE-Glo EX Luciferase assay buffer (Promega). To test response to IGF-1, selected stable pNLCol2 JUN and EV clones were seeded in full medium with 10% FCS, 20,000 cells/well of a 96-well plate. The following day, cells were serum-starved for 16 hr and treated in the presence and absence of 50 nM IGF-1. After 24 hr cells were lysed in ONE-Glo EX Luciferase assay buffer (Promega). Luminescence was measured on a POLARstar Omega plate reader (BMG Labtech), the protein content of the lysate was quantified by Pierce BCA protein assay (ThermoFisher) and luciferase activity was expressed as relative light units per µg protein.

Reverse transcription and quantitative Polymerase Chain Reaction (qPCR)

RNAs were extracted and reverse transcribed using the Pure Link RNA Mini RNA extraction kit (Ambion) and SuperScript III First-Strand Synthesis SuperMix (Invitrogen). ChIP DNAs and cDNAs were amplified using primers shown in Supplementary Table S2 and Sybr Green PCR Mix (Applied Biosystems) on a 7500 Fast RT-PCR System (Applied Biosystems). qPCRs of ChIP DNAs were normalized to input DNA and IgG controls, and qRT-PCRs normalized to ACTB. Results represent 3-5 independent analyses.

Western blotting and Immunoprecipitation

Whole cell extracts were prepared in RIPA buffer with protease and phosphatase inhibitors as above. Cytoplasmic and nuclear proteins were extracted for analysis by western blot using reagents from the Panomics Nuclear Extraction kit as described (5). For immunoprecipitation, nuclear and cytoplasmic proteins were extracted from 40 x 10^6 cells per condition using reagents from the Panomics Nuclear Extraction kit or Active Motif Nuclear Extraction Kit (cat no. 40010). For the latter, cells were swelled in Hypotonic Buffer for 15 min on ice and lysed using kit-supplied detergent (5 µl detergent/100 µl) and vortexing. Nuclei were pelleted by centrifugation (14,000g, 30 sec, 4°C) and lysed in IP buffer (1% Triton X-100, 20 mM Tris pH 7.5, 1 mM EDTA, 100 mM NaCl with protease and phosphatase inhibitors). After centrifugation (14,000g for 5 min at 4°C) to remove insoluble components, 500 µg each extract was pre-cleared for 1hr with IgG and protein A agarose. Pre-cleared extracts were immunoprecipitated overnight at 4°C with 1µg antibody to IGF-1R (#3027, Cell Signaling Technology), RNAPol2 (ab817, Abcam), GATA2 (ab109241, Abcam) or irrelevant antibody (rabbit IgG), collected with protein A agarose and washed repeatedly. Whole cell extracts, nuclear extracts and immunoprecipitates were analyzed by western

blotting as described (5).

IGF-1R immunofluorescence

Serum-starved cells were treated with 50 nM IGF-1 for 30 min in the absence or presence of xentuzumab or Bafilomycin A1. After fixation in 4% paraformaldehyde, 0.1% Triton X-100 in PBS for 20 min, cells were permeabilized in 0.5% Triton X-100 in PBS for 3 min, washed with PBS and blocked in 5% BSA, 0.3% Triton X-100 in PBS for 1 hr. Cells were stained overnight at 4°C with 1:500 IGF-1R monoclonal antibody #9750 (Cell Signaling Technology) in blocking solution. Following PBS washes, bound antibody was visualized using 1:2000 anti-rabbit Alexa fluor-488. After incubation in the dark for 1 hr and further PBS washes, coverslips were DAPI-stained, mounted and visualized as described (5). Total and nuclear IGF-1R signal was quantified using Fiji and expressed as % nuclear IGF-1R in 10-20 cells per condition.

Assays for proliferation, cell survival, motility and migration

Clonogenic survival assays were performed as described in (6). Cell viability was assayed using CellTiter-Blue (Promega), and fluorescence was read on a POLARstar Omega plate reader spectrophotometer (BMG Labtech; 560 nm excitation/590 nm emission). To assay motility, cells were siRNA-transfected, cultured for 72 hr to reach confluence, scratched with a sterile plastic tip and photographed at intervals up to 36 hr. The defect was measured in triplicate wells and expressed as % of the original defect. Results represent ≥3 independent assays. For transwell assays, cells were siRNA-transfected, disaggregated the following day and seeded in RPMI 1640 medium with 0.2% FCS at 10,000 cells/well into inserts of HTS Transwell-96 Permeable Support plates (8.0 µm pore, #3384, Corning). Low serum (0.2% FCS) medium or the same medium containing 50 nM IGF-1 was added to receiver wells. After 24 hr incubation, cell migration into receiver wells was quantified using CellTiter-Blue mixed with Cell Dissociation Solution (Trevigen) and fluorescence was measured on a POLARstar Omega plate reader as above. Results represent 3 independent assays, each with triplicate datapoints.

Supplementary References

1. Dale, OT, T Aleksic, KA Shah, C Han, H Mehanna, DC Rapozo *et al.*, IGF-1R expression is associated with HPV-negative status and adverse survival in head and neck squamous cell cancer. *Carcinogenesis*, **2015**. 36: 648-55.
2. Aleksic, T, AR Worrall, C Verrill, H Turley, L Campo, and VM Macaulay, Improved immunohistochemical detection of type 1 insulin-like growth factor receptor in human tumors. *Immunochem Immunopath*, **2016**. 2: 114.
3. Langmead, B and SL Salzberg, Fast gapped-read alignment with Bowtie 2. *Nat Methods*, **2012**. 9: 357-9.
4. Zhang, Y, T Liu, CA Meyer, J Eeckhoute, DS Johnson, BE Bernstein *et al.*, Model-based analysis of ChIP-Seq (MACS). *Genome Biol*, **2008**. 9: R137.
5. Aleksic, T, MM Chitnis, OV Perestenko, S Gao, PH Thomas, GD Turner *et al.*, Type 1 insulin-like growth factor receptor translocates to the nucleus of human tumor cells. *Cancer Res*, **2010**. 70: 6412-9.
6. Chitnis, MM, KA Lodhia, T Aleksic, S Gao, AS Protheroe, and VM Macaulay, IGF-1R inhibition enhances radiosensitivity and delays double-strand break repair by both non-homologous end-joining and homologous recombination. *Oncogene*, **2014**. 33: 5262-73.
7. Benayoun, BA, EA Pollina, D Ucar, S Mahmoudi, K Karra, ED Wong *et al.*, H3K4me3 breadth is linked to cell identity and transcriptional consistency. *Cell*, **2014**. 158: 673-88.
8. Quinlan, AR and IM Hall, BEDTools: a flexible suite of utilities for comparing genomic features. *Bioinformatics*, **2010**. 26: 841-2.
9. Sehat, B, A Tofigh, Y Lin, E Trocme, U Liljedahl, J Lagergren *et al.*, SUMOylation mediates the nuclear translocation and signaling of the IGF-1 receptor. *Sci Signal*, **2010**. 3: ra10.
10. Jiang, D, Y Zhou, RA Moxley, and HW Jarrett, Purification and identification of positive regulators binding to a novel element in the c-Jun promoter. *Biochemistry*, **2008**. 47: 9318-34.

ChIP primers	
JUN	F: 5′-GACTATACTGCCGACCTGGC-3′ R: 5′AGTTGCACTGAGTGTGGCTG-3′
FAM21A	F: 5′-GAGGTCCCCTCTTTCCAGAC-3′ R: 5′-GGTTCTACCCTAGGTTGGGG-3′
FAM21C	F: 5′-CCTATCCTCCAGCTTCCTCC-3′ R: 5′-ACAGAACCCGCACGTGAT-3′
CCND1	F: 5′-CGGACTACAGGGGAGTTTTGTTG-3′ R: 5′-TCCAGCATCCAGGTGGCGACGAT-3′
β2M	F: 5′-CGGGCTCTGCTTCCCTTAGACT-3′ F: 5′-TGCTAGGACATGCGAACTTAGC-3′
qPCR primers	
JUN	F: 5′- ACGGCGGTAAAGACCAGAAG -3′ R: 5′- CTCGCCCAAGTTCAACAACC -3′
FAM21A	F: 5′- AAAAGGCATATGGAAGCCGGA -3′ R: 5′- ATCTTCCCGATCCGAGTGGA -3′
FAM21C	F: 5′- AAAAGGTGCATCTCTGCTGC -3′ R: 5′- AGCAGCTGTACCCCCAAAAA -3′
ACTB	F: 5′- GATGAGATTGGCATGGCTTT -3′ R: 5′- CACCTTCACCGTTCCAGTTT -3′
EMSA probes	
JUN	F: 5′-BIOTIN-CCACCCTAGAAGATTCTTCTCTGGGCCCGCGGAGGCTCAC GGGATGAGGTAATGCTCCGCTGCCCTCCTACAGTC-3′ R: 5′-GACTGTAGGAGGGCAGCGGAGCATTACCTCATCCCGTGAGCCTCC GCGGGCCCAGAGAAGAATCTTCTAGGGTGG-3′
FAM21A	F: 5′-BIOTIN- AACTCCAGTCCCAGTCCACTTCCGCAGCTTCCTCCCCTCAGC ATGGCAGGTCGGATCACGTGCGGGTTCTGTCACGT-3′ R: 5′- ACGTGACAGAACCCGCACGTGATCCGACCTGCCATGCTGAGGGGA GGAAGCTGCGGAAGTGGACTGGGACTGGAGTT-3′
***JUN* promoter cloning primers**	
JUN promoter	JUN-F: GTTGTT CTCGAG GACGCAGGAAAGGCTTGCA JUN-R: GTTGTT AAGCTT GTTTCGGATCGCCTACACGCT
pNL primers	pNL-F: GGCCTAACTGGCCGGTACCT pNL-R: GGCATCTTCCATGGTGGCTTTA
siRNAs	
Control	AllStars Negative control #SI03650318
JUN	Hs_JUN_2, #SI00034671 Hs_JUN_3, #SI00034678
FAM21A	Hs_LOC387680_1, SI00507584 (FAM21A_1) Hs_LOC387680_2, SI00507591 (FAM21A_2)

Supplementary Table S1: Primers, probes and siRNAs used in this study. ChIP primers were designed to amplify sequences in the proximal promoters of *JUN* on Chromosome 1, and *FAM21A* and *FAM21C* on Chromosome 10 where nuclear IGF-1R showed the greatest enrichment of binding, and also to the promoters of *CCND1* and *B2M*. ChIP inputs were quantified using the same primers. The siRNAs were from Qiagen.

	Median (range)	Number of patients
Age	65 (44 – 74)	137
PSA	6.8 (0.1 – 133)	134
Primary Gleason grade	3	99
	4	38
	5	0
Stage	pT1c	2
	pT2	65
	pT3a	64
	pT3b	6

Supplementary Table S2: Demographics of men treated by radical prostatectomy for prostate cancer. Patients were recruited in Oxford to the Prostate Cancer Mechanisms of Progression and Treatment (ProMPT) study between November 2009 and September 2015, and had FFPE tissue available for IHC. pT, pathological tumor stage. Only one patient in this cohort had died at the time of analysis.

		Membrane IGF-1R		
		IGF-1R < 5	**IGF-1R ≥ 6**	**p-value**
Stage	pT1-2	37	30	0.302
	pT3	32	37	
Gleason grade	6 + 7(3+4)	47	51	0.298
	7(4+3) + 8-9	22	16	
PSA	0-10	50	53	0.154
	> 10	19	11	
		Cytoplasmic IGF-1R		
		IGF-1R < 5	**IGF-1R > 5**	**p-value**
Stage	pT1-2	37	30	0.986
	pT3	68	31	
Gleason grade	6 + 7(3+4)	54	44	0.986
	7(4+3) + 8-9	21	17	
PSA	0-10	58	45	0.972
	> 10	17	13	
		Total IGF-1R		
		IGF-1R ≤ 12	**IGF-1R > 12**	**p-value**
Stage	pT1-2	37	30	0.366
	pT3	33	36	
Gleason grade	6 + 7(3+4)	49	49	0.582
	7(4+3) + 8-9	21	17	
PSA	0-10	54	49	0.930
	> 10	16	14	

Supplementary Table S3: IGF-1R scores and clinical parameters in men undergoing radical prostatectomy for localized prostate cancer. There were no significant associations between clinical parameters and total IGF-1R or IGF-1R in the plasma membrane or cytoplasm. See also Table 1, showing significant association between nuclear IGF-1R and advanced stage, and borderline association of internalized (nuclear plus cytoplasmic) IGF-1R with higher Gleason grade.

	DU145	SK-N-MC
Sample	Total reads (% mapped)	Total reads (% mapped)
IGF-1R + IGF1	10,627,601 (84.7) 9,966,918 (92.5)	8,925,920 (91.9) 11,360,737 (91.4)
IgG	8,586,640 (82.6) 7,800,568 (54.3)	7,313,029 (55.4) 6,522,138 (47.2)
IGF-1R - IGF1	8,515,202 (89.0) 9,075,394 (90.0)	8,657,458 (91.3) 11,199,898 (91.7)
RNAPol2	11,112,074 (95.9)	
H3K4me1	9,987,978 (97.2)	
H3K4me3	13,873,284 (98.3)	

Supplementary Table S4: ChIP-seq: mapped reads. Massively parallel sequencing was performed on duplicate independent samples for IGF-1R ChIP in the absence or presence of IGF-1, and in the negative (IgG) control in each cell line. Individual RNAPol2 H3K4me1 and H3K4me3 ChIP samples were sequenced from DU145 cells. Table shows total number of ChIP-seq reads and % reads mapped to the reference human genome (hg19).

Supplementary Table S5: Genomic locations of IGF-1R binding in DU145 prostate cancer cells. See spreadsheet: Aleksic_Supplementary Table S5.xlsx

Supplementary Figures

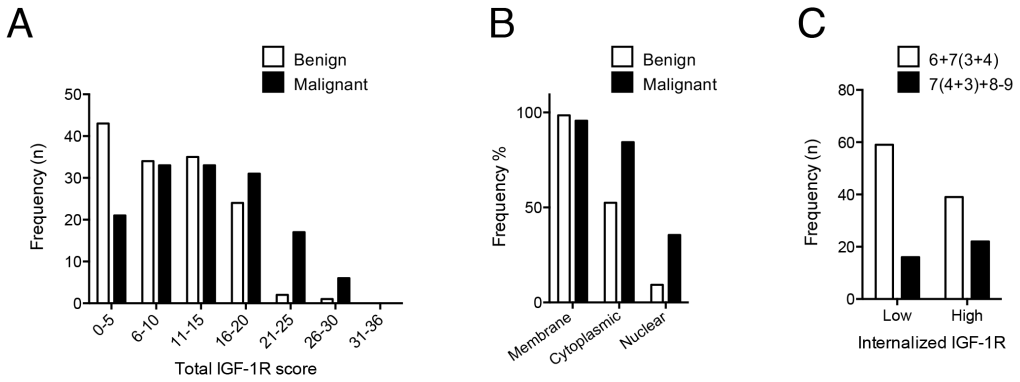

Supplementary Figure S1. Characterization of IGF-1R expression and subcellular localization in prostate cancer. A. Frequency distribution of total IGF-1R by Immunoreactive score in benign and malignant regions of 137 RPs. **B.** IGF-1R signal scored in 137 RPs to generate immunoreactive scores for plasma membrane, cytoplasm and nucleus, as described previously (1, 5). Graph: percentage of tumors containing detectable IGF-1R in each subcellular compartment. **C.** Graph: numbers of prostate cancers containing low (≤6) vs high (>6) internalized (nuclear + cytoplasmic) IGF-1R by grade (n=137). There was borderline association of high internalized IGF-1R with high Gleason grade (p=0.057).

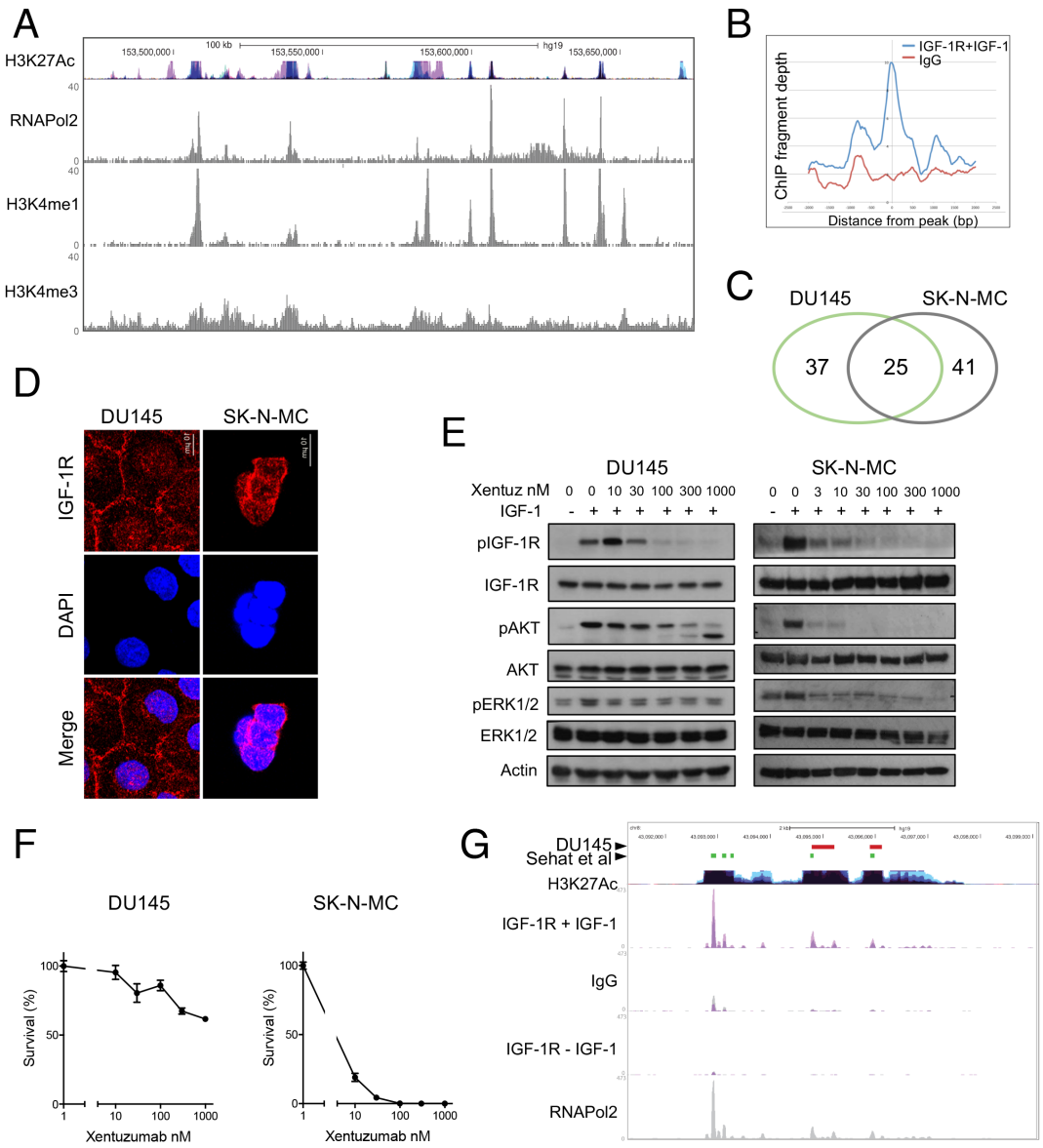

Supplementary Figure S2. IGF-1R ChIP-seq in human cancer cells containing nuclear IGF-1R. A. To delineate transcriptionally active regions, ChIP-seq was performed using antibodies to RNAPol2, H3K4me1 and H3K4me3. Representative UCSC browser image: sharp peaks of DNA binding for RNAPol2 and H3K4me1, and broader peaks of H3K4me3 binding, reported to be associated with increased transcriptional consistency (7). **B.** ChIP fragment depth (per bp per peak) of ChIP-seq-generated peaks from IGF-treated DU145 cells, immunoprecipitated with IGF-1R antibody or IgG. **C.** IGF-1R ChIP-seq peak numbers in DU145 and SK-N-MC cells. **D.** IGF-1R immunofluorescent staining of DU145 and SK-N-MC cells cultured in full medium with 10% FCS, showing detectable membrane IGF-1R in DU145 cells, and punctate nuclear IGF-1R positivity in both cell lines**. E.** In serum-starved DU145 (left) and SK-N-MC cells (right), IGF-1 (50nM, 15min) induced phosphorylation of IGF-1R, AKT and ERK1/2 that was dose-dependently inhibited by xentuzumab. **F.** Clonogenic assays in: left, DU145; right, SK-N-MC cells. Points, bars represent mean ± SEM of 3 assays, each with 3 technical replicates. Xentuzumab induced dose-dependent inhibition of cell survival. SF_{80} values (concentration at which survival equals 80% of control values) were 110 nM (95% confidence intervals 66 – 202 nM) in DU145 and 2.2 nM (2.0 – 2.4 nM) in SK-N-MC. **G.** BEDTools (8) was used to compare peaks of IGF-1R binding in the genomes of DU145 prostate cancer cells (red bars, this report) and DFB melanoma cells (green bars) reported by Sehat et al (9). The only peaks in common were in close proximity to each other in this region of chromosome 8 (43,092,000 to 43,099,000) where our analysis called as peaks two of the 5 peaks reported by (9). These are approximately equidistant from the *HGSNAT* (heparin alpha glucosaminide N-acetyltransferase) gene upstream and the *POTEA* (POTE ankyrin domain family member A) gene downstream.

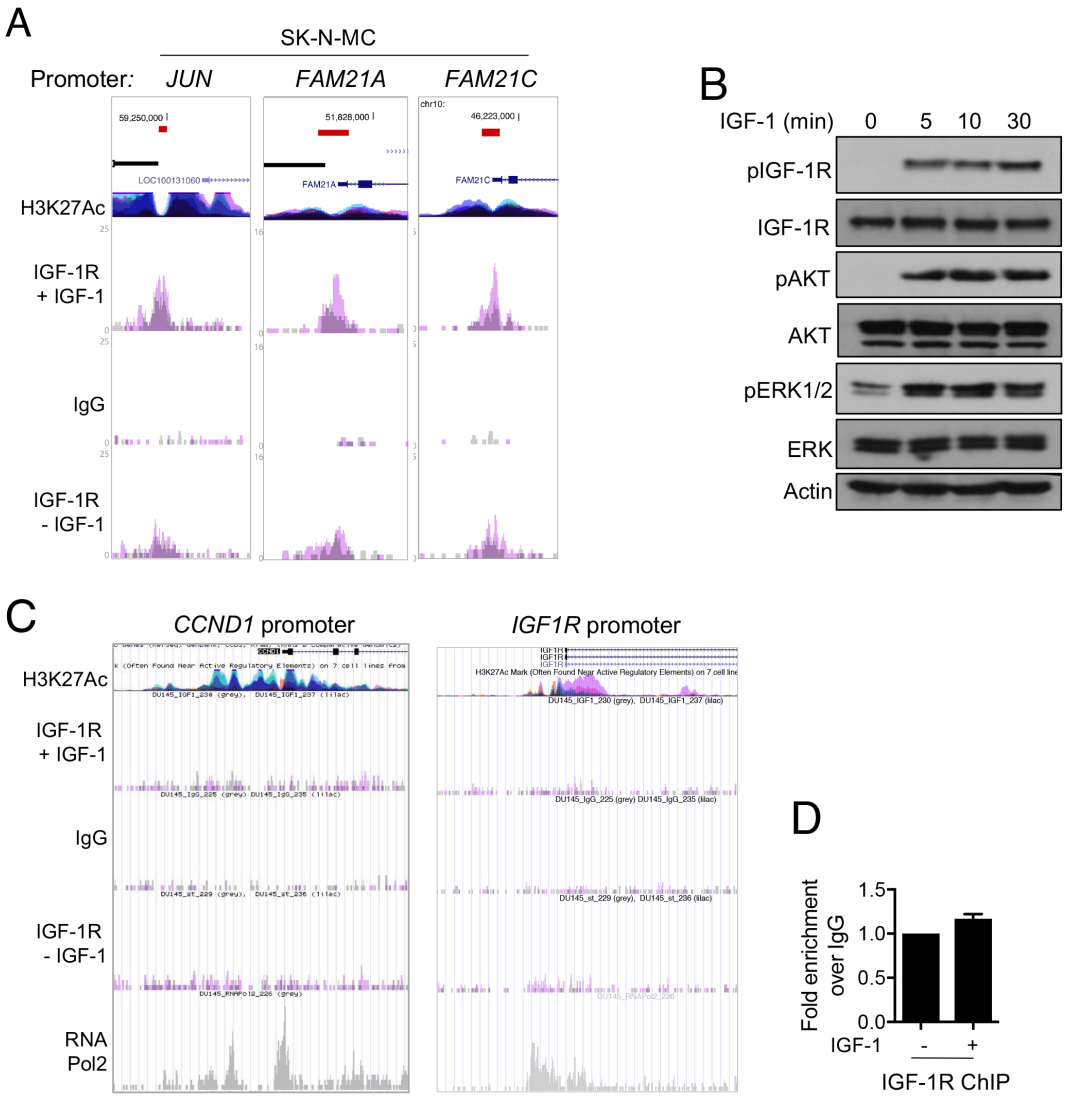

Supplementary Figure S3. ChIP-seq identifies IGF-1R binding peaks in promoters of *JUN* and *FAM21* but not *CCDN1* or *IGF1R*. A. UCSC browser images of ChIP-seq identified peaks of IGF-1R binding in *JUN* and *FAM21A/C* promoters of SK-N-MC cells treated with or without IGF-1 (grey/lilac, duplicate ChIPs), at locations equivalent to sites of IGF-1R recruitment in DU145 cells (Figure 2B). **B**. Serum-starved DU145 cells were treated with 50nM IGF-1 and phosphorylation of IGF-1R, AKT and ERK was assessed by western blotting. **C.** Images from UCSC browser of ChIP-seq in DU145 cells showing proximal promoters of left: *CCND1*, right, *IGF1R*. Both regions contain peak of RNAPol2 binding but no evidence of IGF-1R binding. **D.** IGF-1R ChIP-qPCR for LEF1 binding site in *CCND1* promoter of DU145 cells. Bars: mean ± SEM of 3 independent analyses, each with triplicate technical replicates. showing no enrichment of IGF-1R binding over signal in control (IgG) ChIPs.

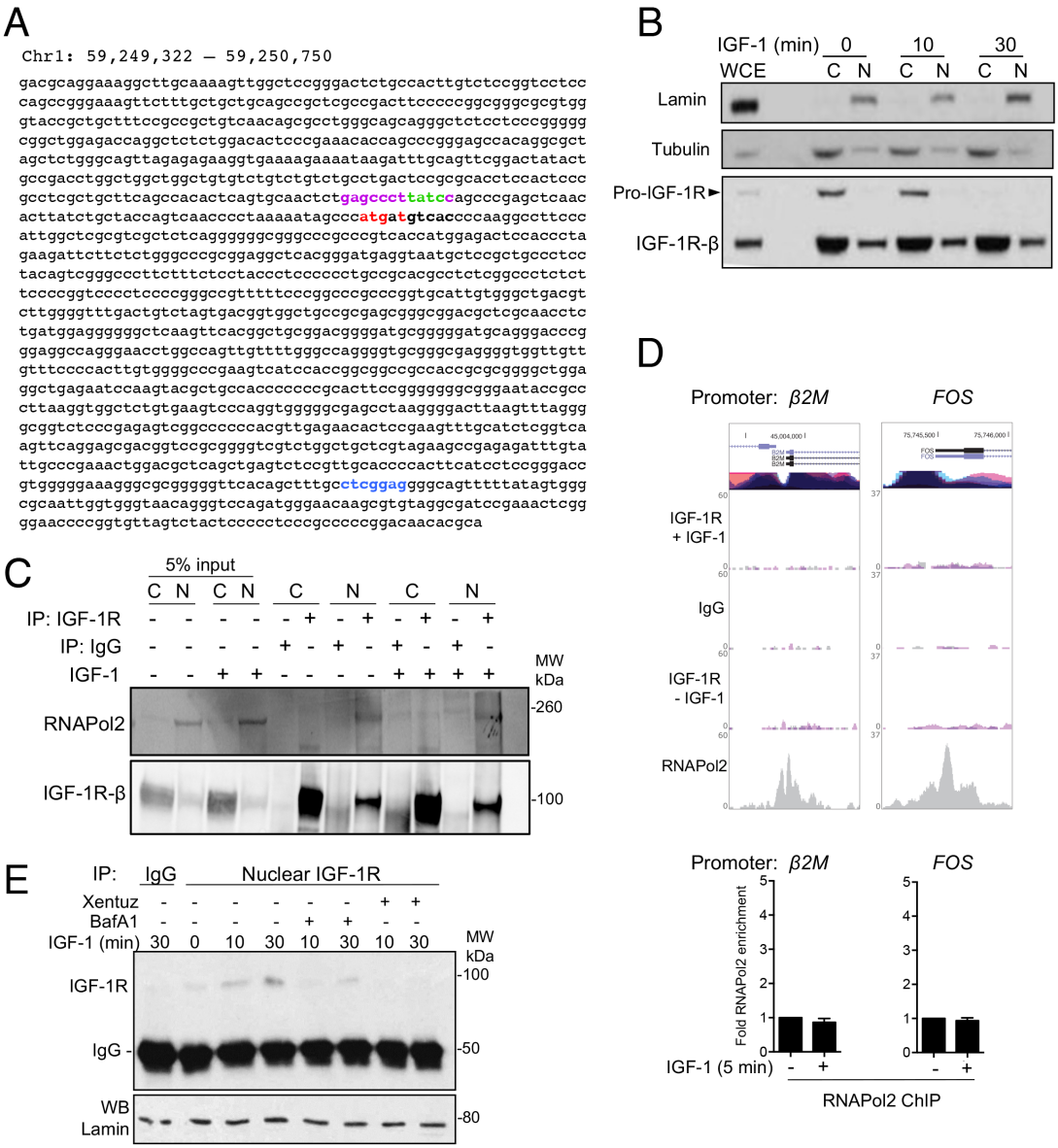

Supplementary Figure S4. Investigating functional consequences of coincidence of IGF-1R and RNAPol2 recruitment to *JUN* and *FAM21A* promoters. **A.** Sequence of IGF-1R binding peak in *JUN* promoter, showing GATA-2 binding site (purple), within which is the TATC = GATA motif (green), the transcription start site and AP-1-like site (red, highly similar to consensus AP-1 site ATGAGTCAT), and GAGCCTC motif (blue) that binds the JUN/KU80 complex (10)**. B.** Nuclear extracts (N) used in co-precipitation experiments (Figure 3D-E) and cytosolic extracts (C) to assess fractionation, in parallel with whole cell extract (WCE). Nuclear extracts were enriched for nuclear protein (lamin) and depleted of cytosolic component (tubulin), also of IGF-1R pro-receptor contained in the non-nuclear fraction. **C.** DU145 cells were serum-starved and IGF-treated for 30 min prior to extraction of cytoplasmic (C) and nuclear (N) proteins from 40 x10^6 cells per condition. IGF-1R IPs or control (IgG) IPs were analyzed by western blotting for RNAPol2 and IGF-1R. **D.** ChIP-seq in DU145 cells showing peak of RNAPol2 but not IGF-1R in promoters of *β2M* (chromosome 15) and *FOS* (chromosome 14). Graphs below: RNAPol2 recruitment to *β2M* and *FOS* promoters was tested in IGF-treated DU145 cells by ChIP-qPCR (mean ± SEM, n=3). RNAPol2 was detected at both promoters but was not enriched by IGF-1. **E.** Nuclear extracts were prepared from DU145 cells treated with 50 nM IGF-1 for 10 or 30 min alone or with 100nM xentuzumab or 50nM Bafilomycin A1 and were used for IGF-1R IP to quantify nuclear IGF-1R. Parallel samples of nuclear extract were western blotted for lamin to confirm equivalence of inputs. Both inhibitors reduced accumulation of IGF-1R in the nucleus.

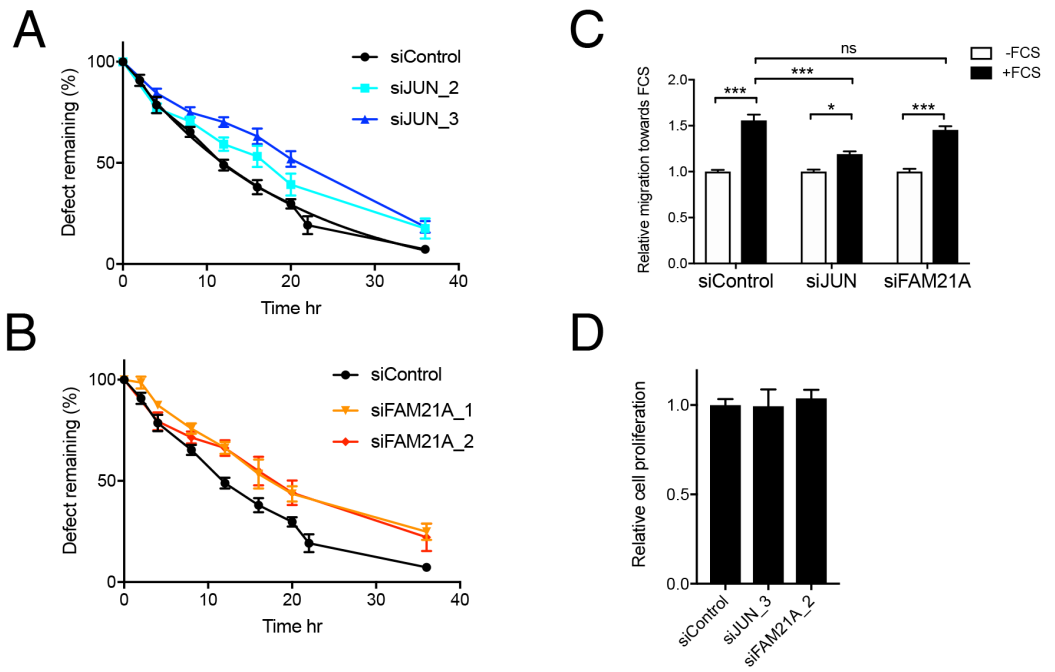

Supplementary Figure S5. Depletion of JUN or FAM21A delays migration towards IGF-1 but has no effect on short-term proliferation. A-B. Migration assays performed as legend to Figure 5C-D, showing pooled data from 5 independent assays each with triplicate data points, expressed as mean ± SEM defect remaining as % of original defect. Data from 12 and 20 hr time points are shown in Figure 5D. **C-D.** DU145 cells were transfected with siControl, siJUN_3 or siFAM21A_2, and the following day: C, re-seeded for transwell migration assays using 10% FCS in receiver wells, otherwise as described in legend to Figure 5E; D, used to assess effects on proliferation during the same time-course as transwell assays, by performing CellTiter-Blue vitality assays after 24 hr.

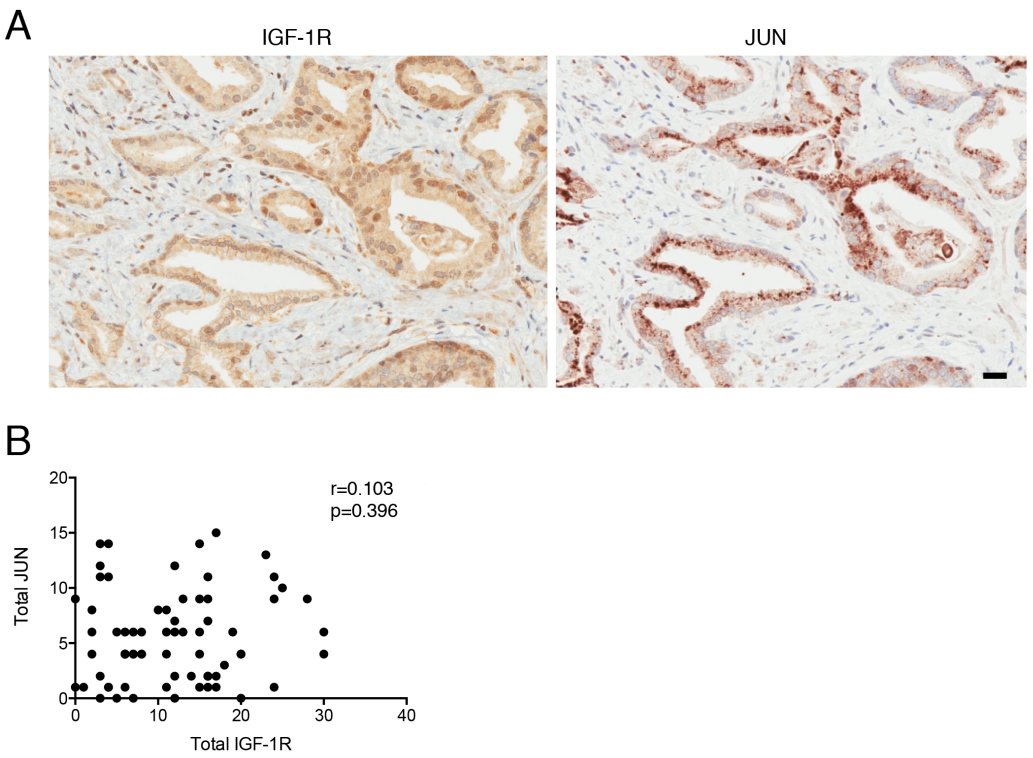

Supplementary Figure S6. JUN expression does not correlate with total IGF-1R in prostate cancer. A. Adjacent RP sections stained for IGF-1R and JUN as Figure 6B, showing Gleason 3+4 pattern invasive cancer (scale bar 30µm). **B.** Total JUN immunoreactive scores in RPs showed no correlation with total IGF-1R (Pearson coefficient for analysis of normally distributed JUN and total IGF-1R scores).